Optik - International Journal for Light and Electron Optics 335 (2025) 172422

Contents lists available at ScienceDirect

Optik

journal homepage: www.elsevier.com/locate/ijleo

Laser-induced nonlinear far-field diffraction patterns of disperse azo dyes

M.Y. Shubar, H.L. Saadon *, M.A. Rahma *

Laser Applications Research Lab, Department of Physics, College of Science, University of Basrah, Basrah, Iraq

ARTICLE INFO

Keywords:
Self-phase modulation
Diffraction ring patterns
Disperse azo dyes
Thermo-optic coefficient
Nonlinear refractive index

ABSTRACT

The nonlinear optical properties of the dispersed azo dyes (orange 3, orange 13 and orange 25) were investigated using laser field-induced spatial self-phase modulation (SSPM) with continuous wave laser of 532 nm. The research of disperse azo dyes at different concentrations and incoming laser power produced diffraction ring patterns. The results of the experiment showed a large nonlinear refractive index n_2 and a large thermo-optical coefficient dn/dT. The effect of excitation laser input and time evolution on shape diffraction pattern shape was investigated. We therefore explain the collapse effect of the diffraction circle model. The results show that the type of laser input is responsible for the variation of the number of diffraction circles. The results indicated that the dispersed azo dyes are a good candidate for use as an optical limiter.

1. Introduction

The interaction between high-performance laser beams and nonlinear optical materials leads to interesting events that highlight the complex relationship between light and matter [1,2]. Laser-induced nonlinear diffraction patterns on distant field diffraction and spatial self-phase modulation (SSPM) are important phenomena to understand how nonlinear optical properties of materials work [3–5]. The effects happen because the medium's intensity-dependent refractive index changes the phase and spatial profile of the laser beam. This leads to effects that can be seen, like diffraction rings or beam reshaping in the far field. Changes in refractive index generated by optical fields can significantly influence laser beam propagation in a nonlinear material. This results in widely recognized. This leads to phenomena such as self-focusing/defocusing and spatial self-phase modulation [6,7]. However, SSPM is recognized as a physical phenomenon that induces self-interference in an emerging beam from the material, resulting in concentric diffraction rings. The exploration of the nonlinear far-field diffraction patterns induced by laser significantly influences the nonlinear optical materials emerged as a significant research area, underlining their potential in photonic applications and advancement technology such as all-optical switching, all-optical limiting, optical signal processing, optical security, and many others [8–22]. With the advance of laser technology, the implications for nonlinear optical materials and photo applications in modern technology are profound [23,24]. These progress promises to revolutionize areas ranging from telecommunications to advanced imaging techniques, reflecting the need for continuous exploration in this field.

In nonlinear optics, azo dyes are a class of organic molecules distinguished by the presence of one or more azo groups (-N = N-) are essential. Because they can absorb a lot of light, stay stable in light, and change forms when exposed to certain wavelengths of light [25–27]. The study of nonlinear optical properties in azo compounds reveals critical intuitions for the next generation optical devices.

* Corresponding authors.
E-mail addresses: haithamsaadon@yahoo.com (H.L. Saadon), mahabct@yahoo.com (M.A. Rahma).

https://doi.org/10.1016/j.ijleo.2025.172422
Received 8 March 2025; Received in revised form 7 May 2025; Accepted 23 May 2025
Available online 24 May 2025

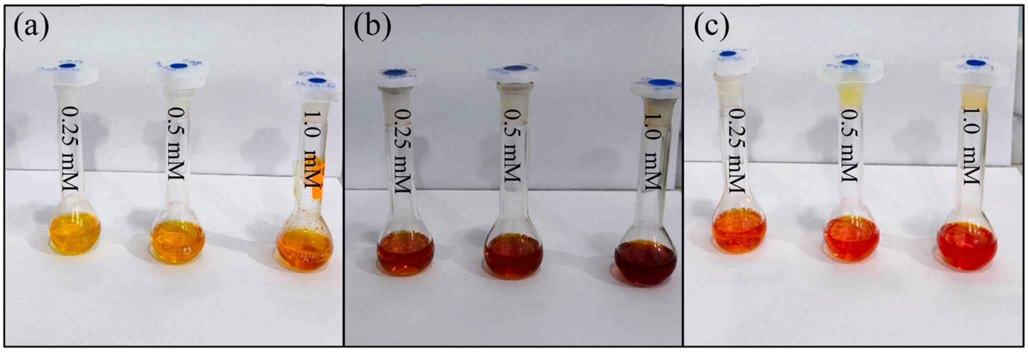

Fig. 1. Photographs of the (a) DO3, (b) DO13, and (c) DO25 dyes solutions.

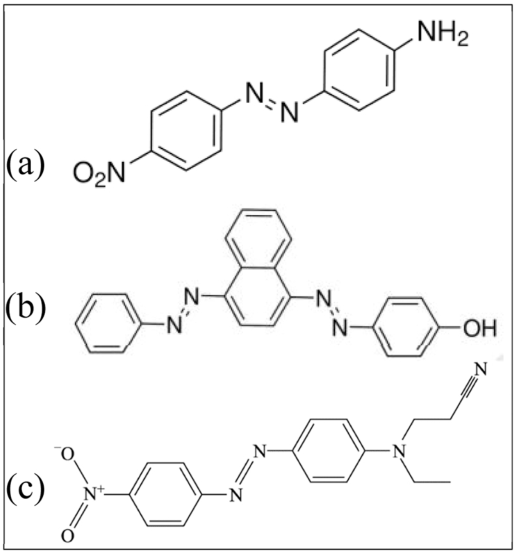

Fig. 2. Chemical structure of (a) DO3, (b) DO13, and (c) DO25 dyes.

Understanding the nonlinear optical properties of azo compounds is essential for the development of efficient optical limits and the improvement of photonic devices. Nonlinear optical refraction and absorption in azo dyes demonstrate promising applications in the optical limiting, essential to protect sensitive devices and light modulators [28–34]. The synthesis of azo compounds demonstrates its nonlinear optical properties, thus validating the potential of these materials under laser excitement. Recently, some materials have been done to demonstrate exceptionally high laser-induced nonlinear optical properties. The effect of SSPM has been used to study different materials [35–38]. Their investigations show good potential applications in nonlinear optical devices.

In the current study, three disperse azo dyes-orange 3 (DO3), orange 13 (DO13), and orange 25 (DO25)-were prepared in solution form. The diffraction ring patterns in the far-field are observed using SSPM method with a laser continuous wave (CW) at 532 nm. Additionally, the relationship between the input laser power and the number of diffraction rings is investigated. DO3, DO13, and DO25 dyes can display interesting nonlinear optical characteristics by altering the quantity of azo dye.

2. Experimental techniques

2.1. Sample preparation

Disperse azo dyes (disperse orange 3, disperse orange 13, and disperse orange 25) were procured from Sigma-Aldrich and utilized without any additional processing. Subsequently, they were dissolved in chloroform at various concentrations of 0.25, 0.5, and 1.0 mM (Fig. 1). The dyes demonstrate solubility in the aforementioned solvent, which is why they were selected for this study. The chemical structure of three dyes represented by DO3, DO13, and DO25 is shown in Fig. 2.

The spectrum of UV–Visible absorption of the DO3, DO13, and DO25 dyes solutions at various concentrations of 0.25, 0.5, and 1.0 mM were illustrated in Fig. 3. The samples show absorption peaks around 520 nm, 440 nm, and 450, respectively, for DO3, DO13, and DO25. Optical energy gap E_g of the dyes was determined using the equation [39]

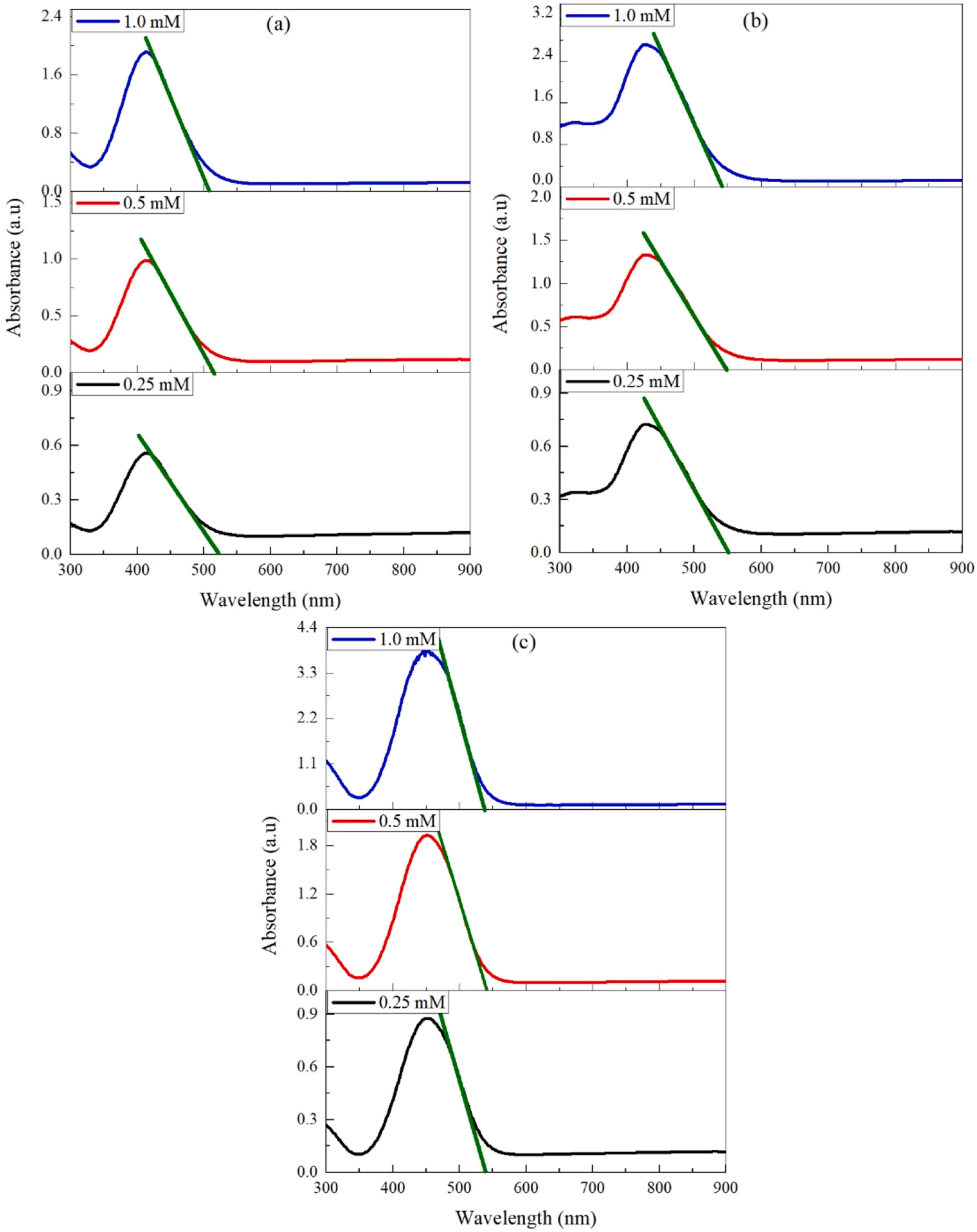

Fig. 3. UV–visible spectrum dyes solution at different concentrations of 0.25, 0.5, and 1.0 mM for materials (a) DO3, (b) DO13, and (c) DO25.

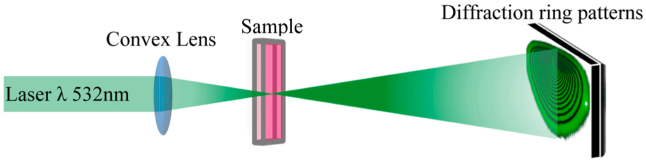

Fig. 4. SSPM experimental setup using CW laser at single laser wavelength of 532 nm.

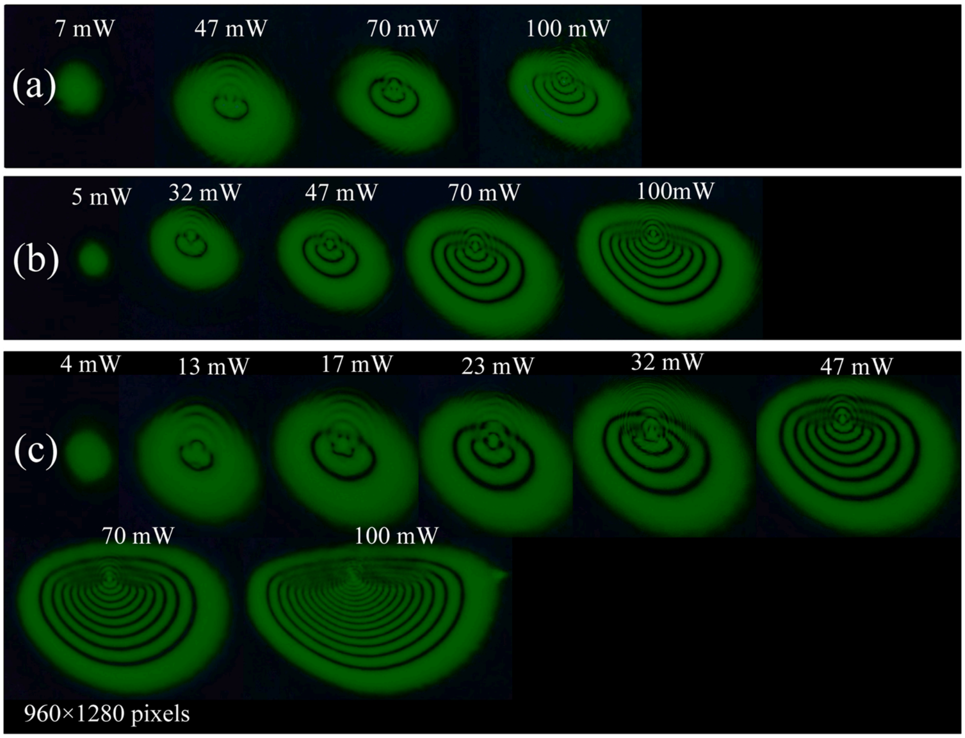

Fig. 5. Diffraction ring patterns of the DO3 dye under different input laser power with different concentrations of (a) 0.25, (b) 0.5, and (c) 1.0 mM.

$$E_g = \frac{1240}{\lambda(nm)} \tag{1}$$

where λ is the wavelength. The energy gap for the dyes DO3, DO13, and DO25 is found to be (2.36, 2.39, and 2.42 eV), (2.25, 2.27, and 2.3 eV), and (2.28, 2.29, and 2.31 eV), respectively, when the concentration increased to 0.25, 0.5, and 1.0 mM. The dye DO13 is more conjugated and delocalized and has minimum energy gap compared to DO25 < DO3.

2.2. Experimental setups

The spatial self-phase modulation (SSPM) experimental setup for capturing far-field self-diffraction ring patterns is depicted in Fig. 4 to determine the nonlinear refractive index n_2. A CW laser pumping solid state (DPSS) in the TEM_{00} mode, with a wavelength of 532 nm, variable output power, and 1.5 mm beam diameter, focused on a 1 mm thickness quartz cell (test) with a 5 cm focal length convex lens. After a laser beam passes through the sample, the self-diffraction ring separates and appears on the screen, and is recorded with the CCD camera. The screen was 70 cm away from the cell. However, our earlier study [28] provided a detailed explanation of the experimental setup.

When the TEM_{00} Gaussian laser beam propagates through a nonlinear material causes a phase distortion on the wavefront of the laser beam, referred known as SSPM effect. Consequently, the nonlinear phase shift $\Delta\Phi$ can be calculated to the number of diffraction rings N as [40,41]

$$N = \frac{\Delta\varnothing}{2\pi} \tag{2}$$

The parameter of nonlinear refractive index n_2 is given by

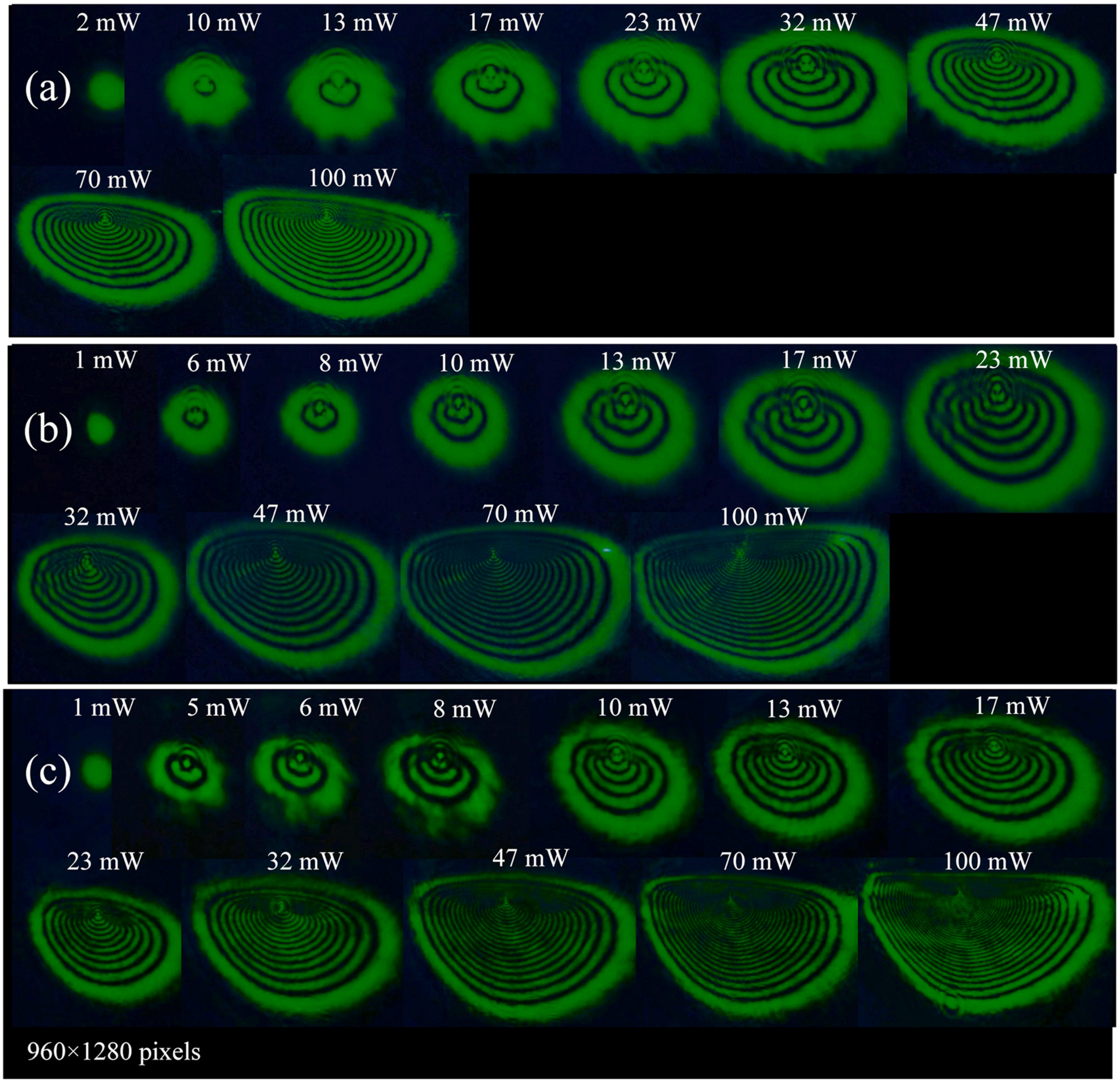

Fig. 6. Diffraction ring patterns of the DO13 dye under different input laser power with different concentrations of (a) 0.25, (b) 0.5, and (c) 1.0 mM.

$$n_2 = \frac{\lambda}{d}\frac{N}{I} \tag{3}$$

where d is the thickness of the sample and I is the laser input intensity. In the context of thermal nonlinearity, the thermo-optic coefficient is given by the following equation [41]

$$\frac{\mathrm{dn}}{dT} = \frac{4n_2\kappa}{\alpha\omega_0^2} \tag{4}$$

where dn/dT is the thermo-optic coefficient, α is the linear absorption, w_0 is the laser beam waist, and κ is the solvent's thermal conductivity.

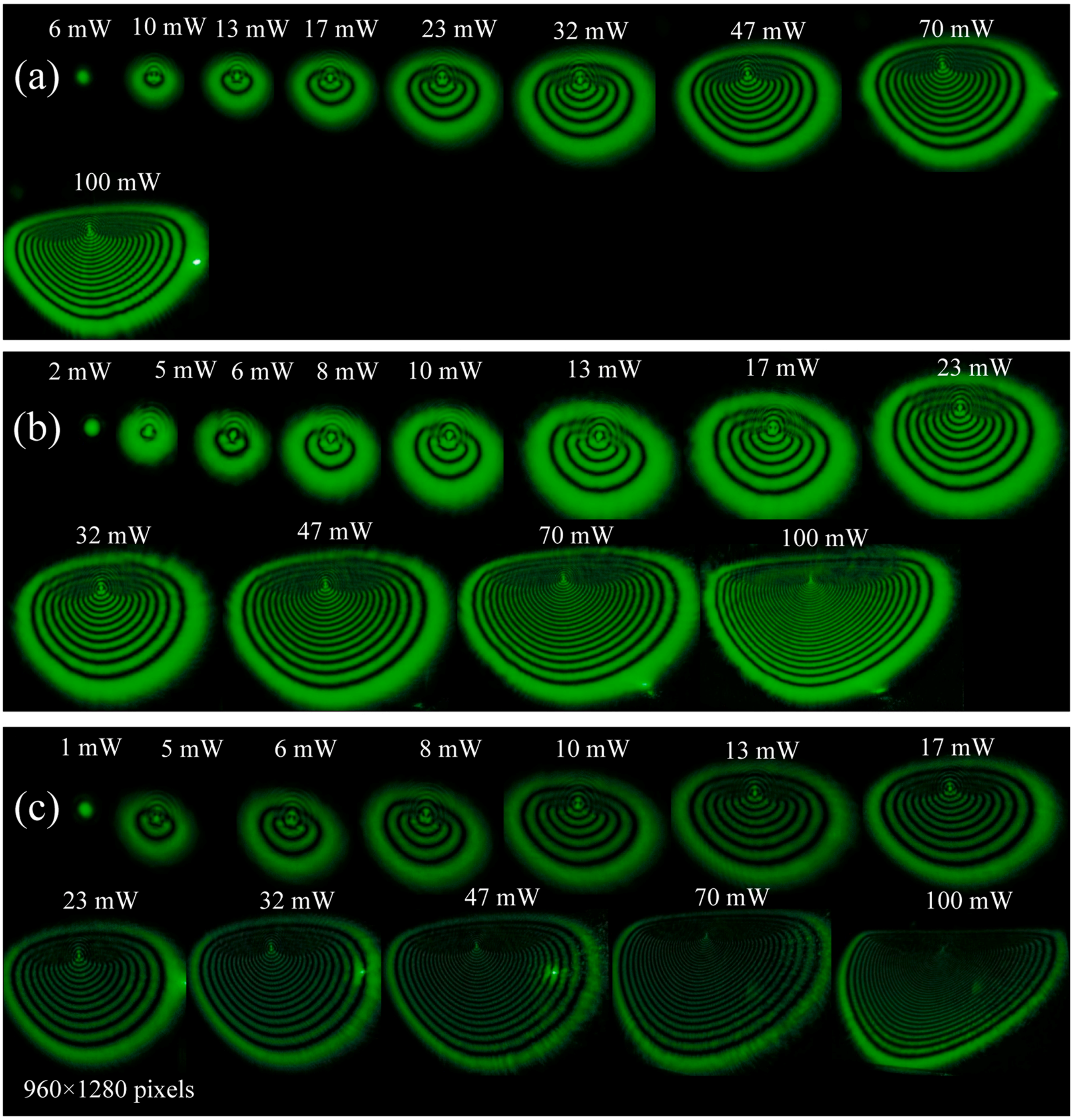

Fig. 7. Diffraction ring patterns of the DO25 dye under different input laser power with different concentrations of (a) 0.25, (b) 0.5, and (c) 1.0 mM.

3. Results and discussions

3.1. The diffraction ring pattern and its dependence on the laser beam intensity

The diffraction ring patterns of DO3, DO13, and DO25 dyes were recorded utilizing the SSPM effect to investigate the effect of varying concentrations from 0.25 mM to 0.5 mM to 1.0 mM, along with different input powers and a 532 nm laser wavelength. Figs. 5–7 present the SSPM diffraction ring patterns for DO3, DO13, and DO25. No ring patterns were observed at power levels below (1–7 mW), (1–2 mW), and (1–3 mW) for DO3, DO13, and DO25, respectively, as indicated by the figures. This is because the laser power is below the threshold required to induce phase shifts for the production of the first ring. At the threshold voltage the first SSPM ring appears. As shown in the figure, with the increasing the input power, the size and quantity of the ring increase gradually. As laser input power increases from 10 to 32 mW, 5–10 mW, and 5–10 mW, DO3, DO13 and DO25, respectively, a phenomenon called SSPM begins to appear on the screen. The pattern increases in size. The distance ring showed the highest intensity, while the inner ring

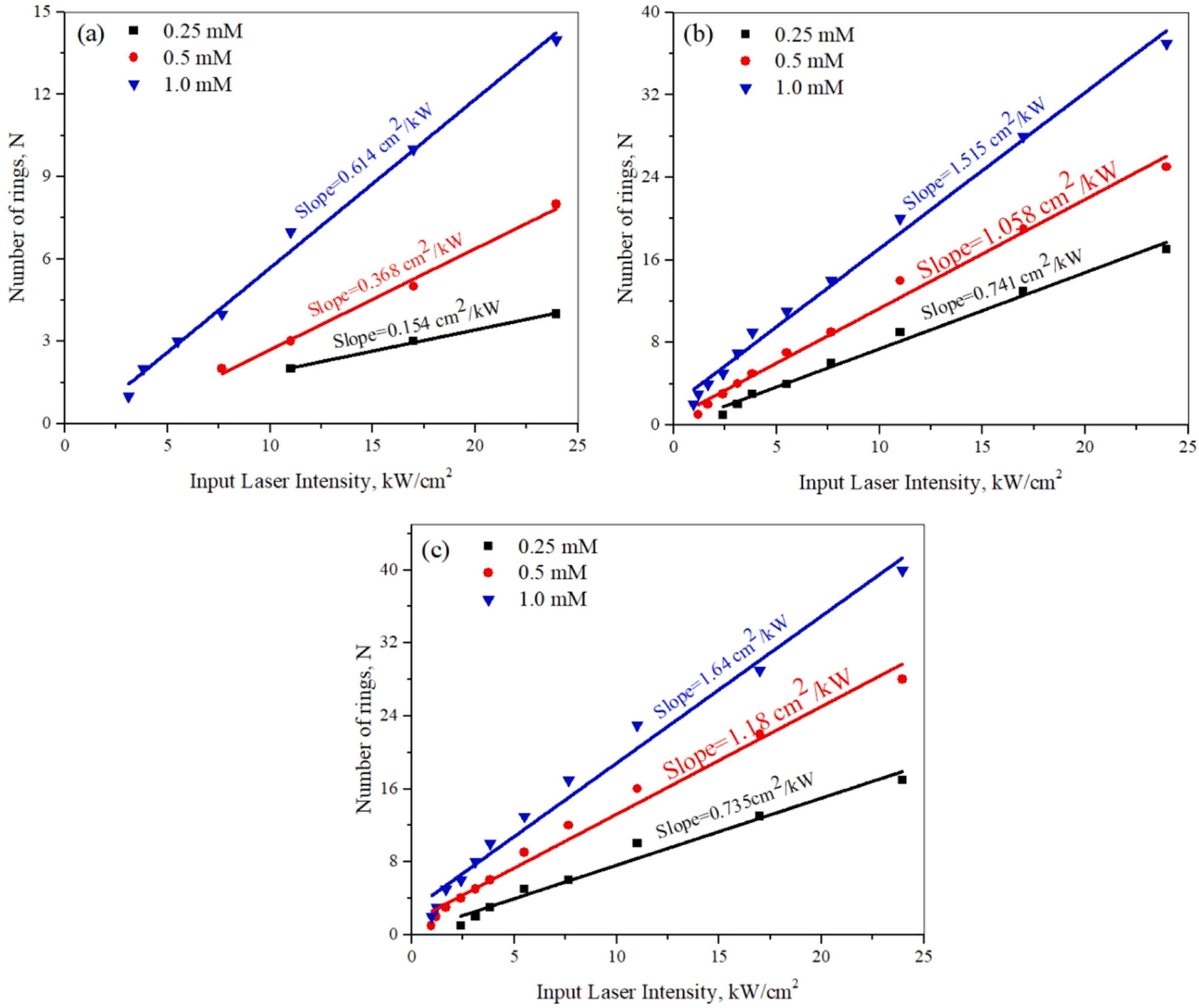

Fig. 8. Dependence of the number of diffraction rings as a function of input laser intensity, I, at different concentrations of 0.25, 0.5, and 1.0 mM for materials (a) DO3, (b) DO13, and (c) DO25.

Table 1
The measured of nonlinear refractive index (n_2) and thermo-optic coefficient (dn/dT) parameters at different materials of DO3, DO13, and DO25.

Material	Concentration (mM)	$n_2 \times 10^{-7}$ (cm^2/W)	$dn/dT \times 10^{-4}$ (K^{-1})
DO3	0.25	0.82	0.26
	0.5	1.73	0.55
	1	3.27	1.03
DO13	0.25	3.94	1.25
	0.5	5.63	1.78
	1	8.06	2.55
DO25	0.25	3.91	1.24
	0.5	6.28	1.99
	1	8.57	2.71

intensity gradually decreased as the pattern moves towards the center. The interference of the upper-level slope light wave, particularly at the Gauss curve inclination point, results in the farthest ring results. The ring patterns corresponded to the shape of the cross-sectional incident laser beams.

To determine the nonlinear refractive index n_2, it is essential to measure the N/I parameter, as indicated in Eq. (3). The N/I parameter denotes the slope of the relationship between the number of diffraction rings N and the laser beam intensity I. Fig. 8 illustrates the relationship between N and I for DO3, DO13, and DO25, respectively. Table 1 displays the important parameters obtained from DO3, DO13, and DO25 at varying concentrations. The data indicate a significant variation in the slopes of the lines corresponding

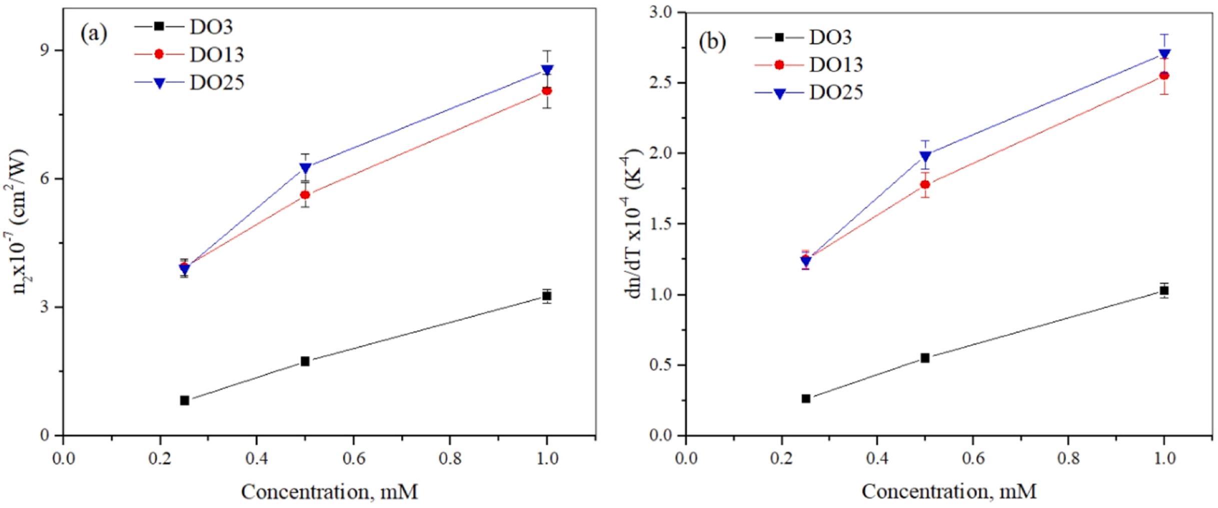

Fig. 9. Variation of the nonlinear refractive index n_2 and thermo-optic coefficient (dn/dT) with concentration under different materials of DO3, DO13, and DO25.

to the materials and concentrations. It is clear that when the concentrations of DO3, DO13, and DO25 increase, the slope value increases for the same material. It is important to highlight that the value of the slopes increasing in the order DO25 > DO13 > DO3 at such concentration. As it can see in Fig. 9, the value of n_2 in Table 1 shows that the optical nonlinearity of the DO25 sample dye is higher than that of the DO13 and DO3. That is the optical nonlinear response increasing in the order DO25 > DO13 > DO3. The characteristics of the material account for this difference. In addition, the DO25 dye has higher thermo-optic coefficient than other materials.

Next, we have determined the thermo-optic coefficient (dn/dT) behavior of the dyes DO3, DO13, and DO25 on input power for various concentrations. For this purpose, we have used the beam waist ω_0 of 26.6 μm and the solvent's thermal conductivity from the literature [42]. Precisely, the linear absorption coefficient for the dyes DO3, DO13, and DO25 was (2.3, 2.8, and 4.1 cm^{-1}), (2.9, 3.92, and 5.76 cm^{-1}), and (3.68, 5.53, and 6.22 cm^{-1}), respectively, when the concentration increased to 0.25, 0.5, and 1.0 mM. The obtained results are given in Fig. 10. As to be noted that the dependence of the thermo-optical coefficient on laser power is strongly influenced by the concentration of the material. Higher concentrations cause nonlinearity, thermal saturation and even permanent changes, whereas lower concentrations behave almost linearly. The design of nonlinear optical materials for high power applications requires an understanding of these phenomena.

Nonlinear refraction can originate physically from electronic, molecular, or thermal sources. The nonlinearity in the current study is thermal in character when a CW laser is used [43]. The obtained findings for the nonlinear refractive index n_2 clearly indicate thermal nonlinearity. Laser beam causes local heating of the material due to light absorption, which alters the refractive index by means of thermal lensing phenomena. As a result, the calculated value of n_2 shows not just the immediate nonlinear electronic response but also a thermal effect that changes the shape of the beam and the ring pattern.

However, it is useful to note that the relative uncertainty of the nonlinear refractive index n_2 measured with the current ring diffraction ring is estimated to be almost 10 %. This estimate was made by applying the law of propagation of relative errors to the Eq. (3) which is produced.

$$\frac{\delta n_2}{n_2} \approx \frac{\delta N}{N} + \frac{\delta I}{I} + \frac{\delta L}{L} \tag{5}$$

Based on the results, it can be deduced that dispersed azo dyes have special nonlinear optical properties that make them especially appropriate for uses like photonic switching and optical image processing applications. Strong electronic polarization by their molecular architectures rich in π-π systems generates high nonlinear refractive index n_2 from which direct control of the beam phase at quite low light intensities is enabled. Moreover, their organic character helps them to produce significant thermal effects from light absorption, which results in clear changes in refractive index by thermal lensing [44–46].

3.2. Comparative study

It can compare these new findings about the DO3, DO13, and DO25 dyes' nonlinear refractive index n_2 with findings from other materials that were made with a 532 nm laser. Table 2 displays the nonlinear refractive index values for DO3, DO13, and DO25 from this study. We compare these values with recently reported values from other materials. The findings show that DO3, DO13, and DO25 have a higher or comparable nonlinear refractive index n_2 at laser wavelength of 532 nm than some other materials. The observed difference may result from the considerable absorbance of the DO3, DO13, and DO25 materials at this wavelength, which is attributed to their high fatty acid content [47]. This comparison indicates that dispersed azo dyes are promising candidates for use as an optical

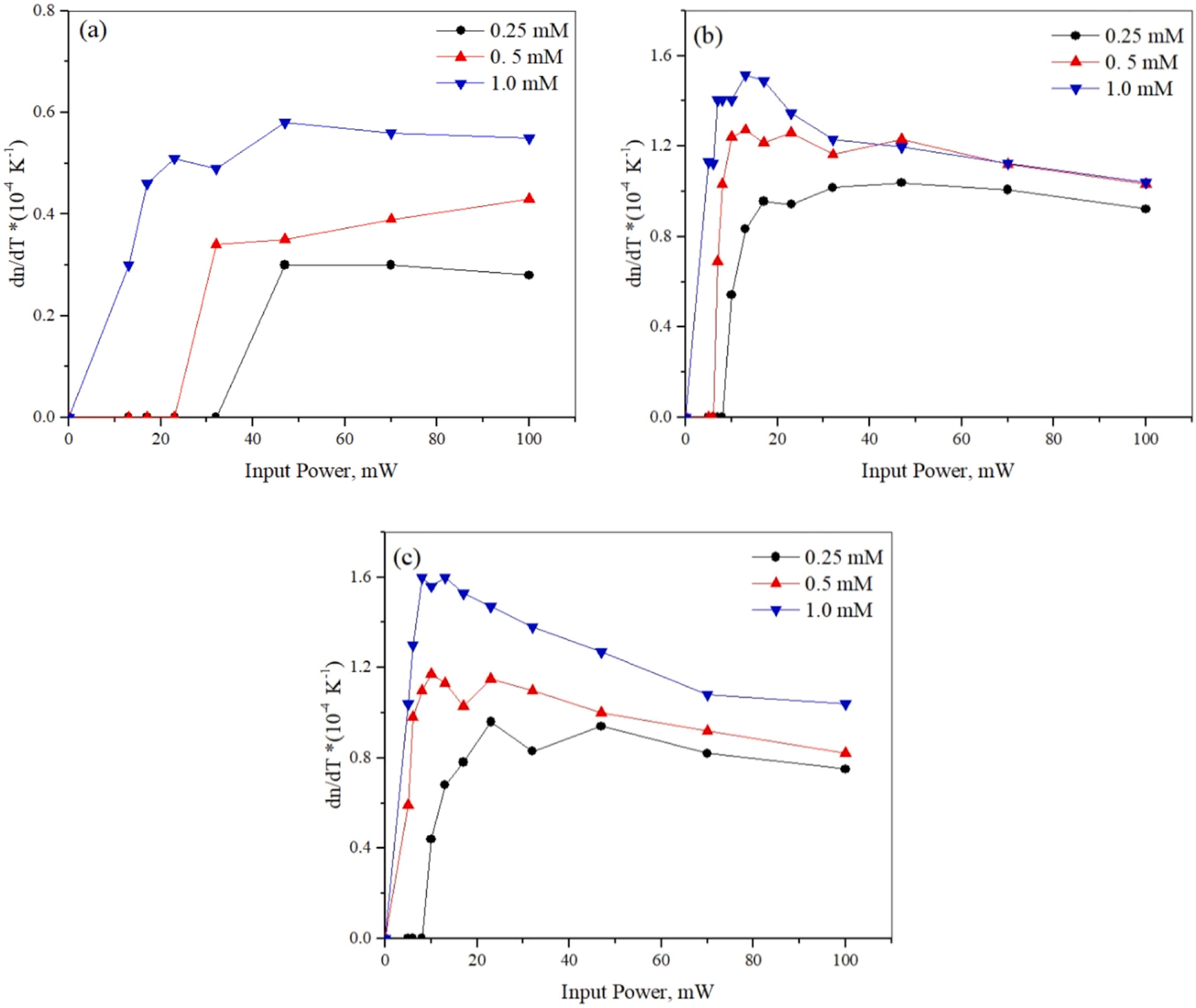

Fig. 10. Effect of increasing laser power on the thermo-optic coefficient (dn/dT) at different concentrations of 0.25, 0.5, and 1.0 mM for materials (a) DO3, (b) DO13, and (c) DO25.

Table 2
Nonlinear refractive index of DO3, DO13, and DO25 measured in the present work and extracted from literature.

Material	$n_2 \times 10^{-7}$ (cm^2/W)	Reference
DO3	1.73	
DO13	5.63	Present work
DO25	6.28	
graphene oxide	0.66	38
acridine orange dye	0.58	39
Basic Violet 16 dye	0.281	40
organotellurium compounds	1.4	25
poly[[(s)−1-(4-nitrophenyl)−2-pyrrolidinethyl]methacrylate]	1.43–3.14	24

limiter.

3.3. Temporal evolution of diffraction rings

Using the SSPM method, Fig. 11 shows how the diffraction rings for DO3, DO13, and DO25 dyes change over time when the laser input power is 70 mW and the concentration is 0.5 mM. The temporal evolution of the diffraction rings can be characterized as follows: No diffraction ring is appear at time = 0 ms. From 53, 44, and 34 ms, for DO3, DO13, and DO25, respectively, to 99, 81, 88 ms, rings

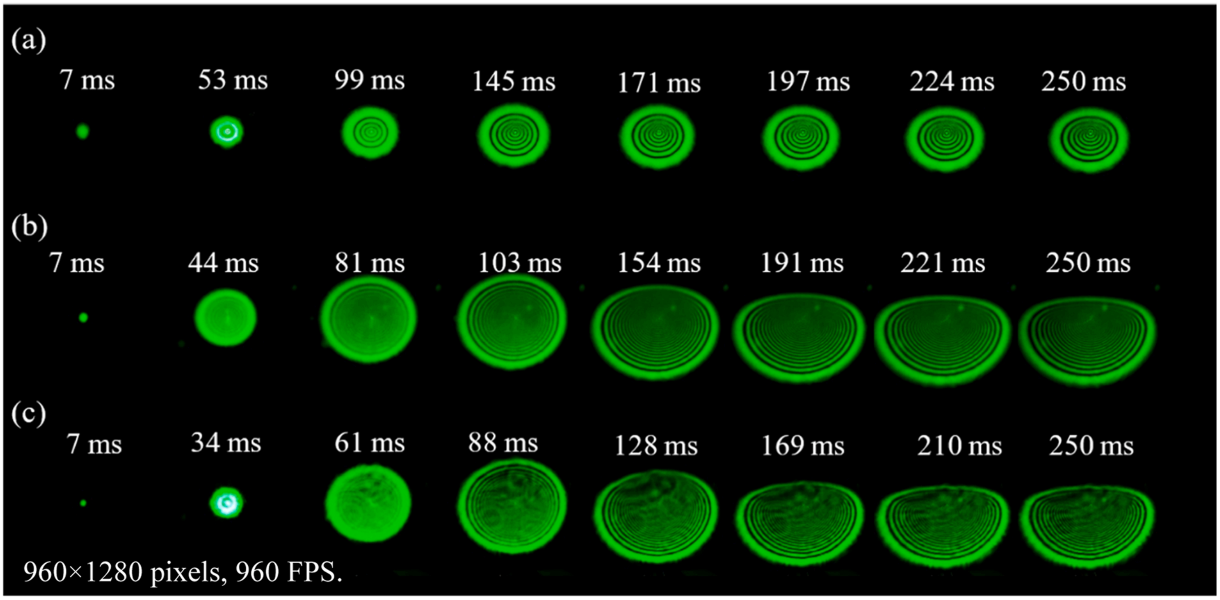

Fig. 11. The temporal evolution of the far-field pattern at input laser power of 70 mW for materials (a) DO3, (b) DO13, and (c) DO25.

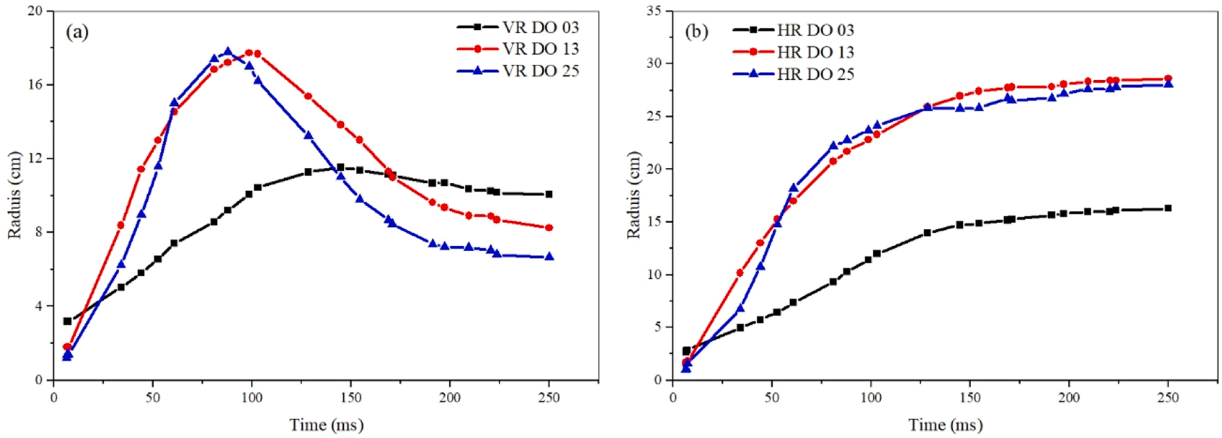

Fig. 12. Radius in the (a) vertical and (b) horizontal of the ring of the laser beam as a function of the exposure time at input laser power of 70 mW under different materials of DO3, DO13, and DO25.

exhibit a symmetrical circular feature, with thermal conduction processes predominating. At times exceeding 145, 103, and 128 ms, the diffraction rings begin to compress vertically in the upper half for DO3, DO13, and DO25, respectively, indicating the onset of the collapse effect in the sample solution. During the time development processes, the vertical compression effect caused by heat convection is the most important one [48] as illustrated in Fig. 12.

Fig. 12 shows the temporal graph showing the diameter of the outermost ring at 70 mW of laser power in vertical and horizontal directions. The diameter of the farthest ring in horizontal and vertical directions increases with time until it reaches a stable size. However, the diameter in the vertical direction diminishes after 145, 103, and 128 ms, of the DO3, DO13, and DO25, respectively. That happened because the refractive index went down, which changed the modulated phase of the laser power in the upper part of the beam. Consequently, the upper section of the ring diminishes, leading to a pattern that appears compressed from the top region.

4. Conclusions

A 532 nm laser wavelength was passed through the orange 3, the orange 13, and the orange 25 dyes. This produces diffraction rings, which can be seen in the far-field using by SSPM. Our work focused on the connection between the laser beam's intensity and the number of diffraction rings at different concentrations. With the help of the new findings, we were able to figure out the nonlinear refractive index n_2 (about 10^{-7} cm^2/W) and the thermo-optic coefficient dn/dT. The collapse effect was observed when the time evolution of the diffraction rings was recorded with the change of the laser power of the input. The large value of its nonlinear refractive index suggests promising materials for all-photonic switching and image processing.

CRediT authorship contribution statement

M.Y. Shubar: Data curation. **H.L. Saadon:** Writing – original draft. **M.A. Rahma:** Formal analysis.

Declaration of Competing Interest

The authors declare that they have no known competing financial interests or personal relationships that could have appeared to influence the work reported in this paper.

Data availability

Data will be made available on request.

References

[1] R.W. Boyd. Nonlinear Optics, 4th ed., Academic Press, 2020.
[2] D.N. Papadopoulos, et al., Nat. Photonics 10 (2016) 123–130.
[3] X. Zhu, B. Dong, Opt. Exp. 23 (2015) 14036–14045.
[4] L. Hu, F. Sun, H. Zhao, Crystals 13 (2023) 271.
[5] T. Neupane, B. Tabibi, W.J. Kim, F.J. Seo, Crystals 13 (2023) 271.
[6] X.J. Zhang, Z.H. Yuan, R.X. Yang, Y.L. He, Y.L. Qin, Cent. South Univ. 26 (2019) 2295–2306.
[7] X. Yang, D. Li, Q. Li, X. Meng, Appl. Opt. 59 (2020) 10069–10075.
[8] M.Y. Shubar, H.L. Saadon, S.J. Abbas, Mater. Technol. 35 (2020) 494–506.
[9] M.A. Rahma, H.L. Saadon, M.A. Mahdi, J. Phys. D: Appl. Phys. 50 (2017) 135103.
[10] M.A. Rahma, H.L. Saadon, M.A. Mahdi, AIP Conf. Proc. 2977 (2023) 040103.
[11] M.A. Rahma, H.L. Saadon, Non Opt. Quant. Opt. 59 (2024) 227–236.
[12] M.A. Rahma, H.L. Saadon, AIP Conf. Proc. 2190 (2019) 020031.
[13] M.A. Rahma, H.L. Saadon, M.A. Mahdi, Optik 174 (2018) 580–590.
[14] K. Ogawa, T. Zhang, K. Yoshihara, Y. Kobuke, J. Am. Chem. Soc. 124 (2002) 22.
[15] F. Rößler, T. Kunze, A.F. Lasagni, Opt. Express 25 (2017) 22959.
[16] E.A. Mohammed, H.L. Saadon, J. Phy: Conf. Ser. 1234 (2019) 012037.
[17] H.L. Saadon, N. Théofanous, M. Aillerie, J.P. Salvestrini, M.D. Fontana, J. Opt. A: Pure Appl. Opt. 8 (2006) 677–682.
[18] S. Jiao, J. Liu, L. Zhang, F. Yu, G. Zuo, J. Zhang, F. Zhao, W. Lin, L. Shao, Opto-Electron. Sci. 1 (2022) 220010.
[19] H. Amed, A. Mohmoud, M. Mobarak, H. Mhmoud, A. El-salam, T. Mohamed, J. Mol. Liq. 340 (2021) 117199.
[20] F.A. Samad, A. Mahmoud, M.E. El-Kouly, R. Apsari, T. Mohamed, J. Mol. Liq. 418 (2025) 126679.
[21] M.E. El-Kouly, A.M. Kobaisy, H. Ahmed, T. Mohamed, Opt. Quant. Electron 55 (2023) 941.
[22] Y. Abd. El-Salam, H.D. Adday, F.A. Samad, H. Qayyum, T. Mohamed, Nanomaterials 14 (2024) 1290.
[23] Q. Wu, L. Peng, Z. Huang, X. Liu, M. Luo, D. Gao, H. Meng, Light.: Sci. Appl. 14 (97) (2025) 1–29.
[24] O. Aljohani, I. Dierking, Front. Mater. 11 (2024) 1453744.
[25] R. Ganjoo, Ch Verma, As Kumar, M.A. Quraishi, Adv. Coll. Inter. Sci. 311 (2023) 102832.
[26] L.D. Ardila-Leal, R.A. Poutou-Piñales, A.M. Pedroza-Rodríguez, B.E. Quevedo-Hidalgo, Molecules 26 (2021) 3813.
[27] H. Zollinger. Color Chemistry: Syntheses, Properties, and Applications of Organic Dyes and Pigments, 3rd ed., Wiley-VCH, 2023.
[28] H.L. Saadon, Opt. Quant. Elect. 48 (2016) 1–8.
[29] H.L. Saadon, B. Ali, A.A. Al-Fregi, Opt. Laser Technol. 58 (2014) 33–38.
[30] S.S. Suvidha, C.S. Mavila, S. Chitrambalam, I. Hubert Joe, N. Sekar, Polycycl. Aromat. Compd. 41 (2021) 1431–1548.
[31] H. Motiei, A. Jafari, R. Naderali, Opt. Laser Technol. 88 (2017) 68–74.
[32] S. Jeyaram, T. Geethakrishnan, J. Fluoresc. 30 (2020) 1161–1169.
[33] M.K. Sadigh, M.S. Zakerhamidi, Opt. Laser Technol. 100 (2018) 216–224, 2018.
[34] M. Yahya, N. Seferoğlu, G. Kaplan, Y. Nural, A. Barsella, Z. Seferoğlu, J. Mol. Struct. 1273 (2023) 134257.
[35] A. Ghanem, M.D. Zidan, M.S. EL-Daher, Results Opt. 9 (2022) 100268.
[36] M.D. Zidana, M.M. Al-Ktaifanib, M.S. EL-Daherc, A. Allahhama, A. Ghanem, Opt. Laser Technol. 131 (2020) 106449.
[37] M.D. Zidan, M.S. EL-Daher, M.M. Al-Ktaifani, A. Allahham, A. Ghanem, Optik 219 (2020) 165275.
[38] A.J. Almusawe, M.A. Rahma, H.L. Saadon, Ali Q. Abdullah, Ali F. Marhoon, Phys. Scr. 99 (2024) 115519.
[39] S.H. Housavi, T.S. Müller, P.W. de Oliveira, J. Mater. Sci: Mater. Electron 24 (2013) 3338.
[40] Y. Shan, J. Tang, L. Wu, S. Lu, X. Dai, Y. Xiang, J. Alloy Comp. 771 (2019) 900.
[41] O.R. Vol, K. Ogusu, Y. Kohtanl, H. Shao, Opt. Rev. 3 (1996) 232.
[42] R.H. Perry, D.W. Green. Perry's Chemical Engineers' Handbook, 8th Ed., McGraw-Hill, New York, 2008.
[43] N. Demetrios, L.C.K. Christodoulides, J.S. Gregory, I.S. George, Opt. Photo J. 2 (2010) 60.
[44] Y. Pan, Z. Lyu, C. Wang, Opt. Contin. 4 (2021) 2714–2720.
[45] Lu Wen-Qiang, Chen Gui-Ying, Hao Zhao-Feng, Xu Jing-Jun, Tian Jian-Guo, Zhang Chun-Ping, Chin. Phys. B 19 (2010) 084208.
[46] H. Rashidnejad, H. Motiei, M. Ramezanitaghartapeh, A. Ng, Kay Lup, J. Photochem. Photobiol. A 426 (2022) 113763.
[47] K.E. Kaylegian, J.M. Lynch, J.R. Fleming, D.M. Barbano, J. Dairy Sci. 92 (2009) 2485–2501.
[48] Y. JIA, Y. Shan, L. WU, X. Dai, D. Fan, Y. Xiang, Photon. Res. 6 (2018) 1040–1047.